Materials Research. 2014; 17(6): 1384-1390
DOI: http://dx.doi.org/10.1590/1516-1439.281214

Morphological and Electrical Evolution of ZnO:Al Thin Films Deposited by RF Magnetron Sputtering onto Glass Substrates

Érica Pereira da Silva[a], Michel Chaves[a], Steven Frederick Durrant[a], Paulo Noronha Lisboa-Filho[b], José Roberto Ribeiro Bortoleto[a]*

[a]Technological Plasmas Laboratory, São Paulo State University – UNESP, Av. Três de Março, 511, Alto da Boa Vista, CEP 18087-180, Sorocaba, SP, Brazil
[b]Group of Advanced Materials, São Paulo State University – UNESP, Av. Eng. Luiz Edmundo Carrijo Coube, 14-01, Núcleo Habitacional Presidente Geisel, CEP 17033-360, Bauru, SP, Brazil

Received: March 22, 2014; Revised: September 11, 2014

In this work, the surface and electrical characteristics ZnO:Al thin films deposited by RF magnetron sputtering onto glass substrates have been investigated. Analysis of surface morphologies revealed two growth stages. In the first stage, up to thicknesses of 100 nm, the films show surface structures with a granular form without preferential orientation. Beyond thicknesses of 100 nm, however, the grain structures increase in size and height, producing a pyramidal form and preferred orientation along the *c*-axis. The XRD results show that the films have a preferred orientation in the (002) plane. Furthermore, with the evolution of the film thickness the electrical resistivity decreases to a minimum of 1.6×10^{-3} Ω cm for the film of 465 nm thickness. The doping with aluminum atoms produces an increase in concentration of charge carriers to around 8.8×10^{19} cm^{-3}. All films exhibit high optical transmittance (above 85%) in the visible region.

Keywords: *ZnO:Al, RF magnetron sputtering, surface morphology, optical transmittance, electrical resistivity*

1. Introduction

Transparent conductive oxides (TCOs) are fundamental components in optoelectronic applications[1-3]. TCO materials have the ability to couple two important features for applications in the optoelectronic devices industry; an optical transmittance of around 80% in the visible region and low electrical resistivity of around 10^{-3} to 10^{-4} Ω cm[1-3]. Indium tin oxide (ITO) is currently the most widely used TCO for optoelectronic devices. However, indium, the main chemical component of ITO, is scarce in nature and consequently the production cost of ITO is relatively high[3-5]. Therefore, there is an incentive to find an alternative to ITO.

Zinc oxide (ZnO), a promising alternative to ITO, is an n-type semiconductor and, can therefore easily be doped with group III elements, such as aluminum and gallium. The advantages of ZnO include an optical gap of 3.3 eV, low toxicity, good optical and electrical properties, and chemical stability in plasma processes[1-3]. In addition, zinc is abundant in nature; consequently, ZnO is relatively cheap.

ZnO:Al and ZnO:Ga thin films have been produced by a wide variety of techniques, including chemical and physical processes, such as pulsed laser deposition[6], chemical vapor deposition[7], spray pyrolysis[8], sol-gel technique[9], atomic layer deposition[10] and magnetron sputtering[11] onto a variety of substrates. Among these methods, magnetron sputtering is especially interesting, because it can not only be conducted at low temperatures, but can also produce high-quality crystalline intrinsic and doped ZnO thin films[12]. Moreover, this technique allows the deposition of thin films on large areas of substrate.

The surface morphology of a thin film may indicate its dynamic growth[13-15]. Typically, growth of a thin film is a non-equilibrium process, which can lead to the formation of a roughened surface with granular or pyramidal structures[4,13,15]. Moreover, the properties of the surface of a thin film, especially the surface roughness, may strongly influence their applications[4,13,16]. There are also intrinsic relations between the surface morphology and other factors, such as crystalline structure and film thickness, which have been found to play important roles in determining physical and chemical film properties[15,17].

Films having a high native surface roughness can be beneficial for light trapping in solar cell applications[16]. In other applications, however, different thickness/roughness ratios are required; for example, smooth surfaces are preferred for electronic devices[18]. This makes the understanding the surface evolution and its correlation with electrical and optical properties mandatory for specific ZnO thin film applications. In this work, aluminum-doped zinc oxide thin films were grown on glass substrates using reactive RF magnetron sputtering of a zinc-aluminum target. The surface evolution of the films and their optical and electrical properties were investigated as a function of film thickness.

*e-mail: jrborto@sorocaba.unesp.br

2. Experimental

The deposition system consists of a cylindrical 304 stainless steel chamber of 270 mm diameter and 200 mm in height. Films of ZnO:Al were deposited on 1mm-thick glass substrates by RF magnetron sputtering. Before loading in the sample holder the glass substrates were ultrasonically cleaned in deionized water with detergent (Det limp S32) for 8 min. After that the substrates were subjected to a second ultrasound bath containing only distilled water, and finally the substrates were subjected to an isopropyl alcohol bath. A metallic zinc-aluminum (1 wt% of Al) target of 99.99% purity was used. The plasma was maintained using a forward 13.56 MHz (RF) power of 100 W. In all depositions the substrate-holder was polarized. An argon pressure of 6.7 Pa was employed. A substrate temperature of 373K was maintained during the growth. To study the growth evolution, different ZnO:Al films with thicknesses ranging from 0 up to 465 nm were deposited.

Surface morphology was measured using atomic force microscopy (AFM, XE-100, Park Systems) operating in air. The scanned area was 2 mm × 2 mm with 512 × 512 pixels. The parameters of surface roughness (σ) and correlation length (ξ) were obtained from the surface morphology measured using AFM. Surface roughness is mathematically defined by Equation 1[19].

$$\sigma = \sqrt{\frac{1}{N}\sum_{i=1}^{N}\left(h_i - \langle h \rangle\right)^2} \quad (1)$$

In this equation N is the number of pixels, h_i the individual heights, and <h> the mean height.

Furthermore, the average value of correlation length ξ was derived by fitting by a Lorentzian curve to the power spectral density (PSD) calculated from AFM images. The correlation length ξ is usually related to the lateral size evolution of the surface structures.

Optical transmittance spectra were obtained using a Uv-Vis-NIR spectrometer (Lambda 750, Perkin Elmer) over the 190 nm to 3300 nm wavelength range. The electrical resistivity was measured by the four-point probe method at room-temperature. An X-ray diffractometer (D/MAX-2100/PC, Rigaku) was used to determine the degree of crystallinity of the ZnO thin films.

3. Results and Discussions

Table 1 shows the values of morphological, optical and electrical properties obtained for the ZnO:Al films as a function of film thickness.

Figure 1 allows comparison of XRD spectra obtained for the film of ZnO:Al (of thickness 465 nm) and of the intrinsic ZnO film. The intrinsic ZnO film was also obtained by RF magnetron sputtering, and possesses a thickness of 550 nm. Both the ZnO:Al film (465 nm) and the intrinsic ZnO film exhibit a preferred orientation along the *c*-axis, perpendicular to the substrate surface in the plane (002), which, according to the JCPDS (65-3411) table, corresponds to a wurtzite ZnO structure.

The average crystallite size parallel to the film surface can be estimated by an analysis of the full width at half maximum (FWHM) and maximum peak position, as observed in the XRD spectra, using Scherrer's equation[20]:

$$\tau = \frac{K\lambda}{\beta\cos\theta} \quad (2)$$

where *K* represents a shape factor, that normally has a value of 0.9[20], λ is the wavelength of the X-rays, β is the value of the FWHM of the (002) plane peak and θ corresponds to the Bragg angle. The incident wavelength used was 1.5405 Å. Using the data in Scherrer's formula the average crystallite size (τ) of the intrinsic ZnO film was found to be 17.7 ± 0.1 nm. When the film was doped with aluminum, however, the crystallite size decreased to 8.1 ± 0.1 nm. Furthermore, it is clear from observation of Figure 1 that the intensity of the peak corresponding to the (002) plane decreased with doping, while the FWHM value roughly doubled.

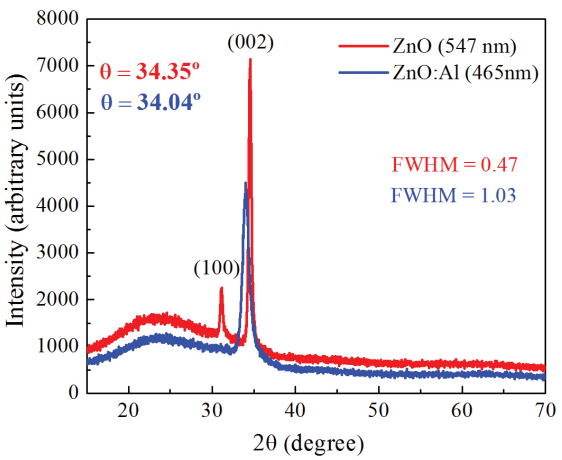

Figure 1. XRD spectra of intrinsic ZnO and ZnO:Al films deposited onto glass substrates.

Table 1. Structural, electrical and optical properties of the ZnO:Al thin films as a function of the thickness.

Properties/Sample	Substrate	S1	S2	S3	S4	S5	S6
Thickness (nm)	0	25	50	100	185	250	465
Roughness (nm)	1.71	2.10	2.26	5.3	8.3	9.9	19.5
Correlation length (nm)	0.11	0.072	0.067	0.094	0.14	0.16	0.29
Resistivity (10^{-3} Ω cm)	--	--	8.6	5.7	1.8	1.6	1.6
Refractive index at 550 nm	1.51	2.01	2.09	2.1	2.10	2.06	2.0
Transmittance at 550 nm (%)	91.6	91.5	88.8	83.8	85.8	85.9	84.7

It may be noted from the diffraction spectra that there is a difference in the values of the Bragg angle. The (002) plane of the intrinsic ZnO film is attributed to the peak at θ = 34.35°, close to the default value given in the JCPDS table (θ = 34.43°). The peak attributed to the (002) plane of the ZnO:Al film, however, appears at smaller angles (θ = 34.04°). The presence of residual compressive stress in the crystal lattice of ZnO, inferred from the reduction in θ, influences the dynamic growth of the grains.

Figure 2 shows AFM surface images of the ZnO:Al films of different thicknesses deposited onto glass substrates. The surface morphology is found to evolve homogeneously with well-distributed structures. Initially, the surface morphology is mainly formed by small granular structures. Beyond film thicknesses of about 100 nm, these structures increase in both height and width, until faceted structures are produced.

As shown in Figure 3, AFM images obtained for the films with thicknesses of 50 nm and 250 nm show the differences between the surface structures. The lateral profile obtained for each image makes clear the growth of the structures in both height and width. Similar behavior has been reported by Vasco et al for ZnO/InP (100) films grown by PLD technique[15]. The same authors also reported the presence of two growth stages. In the first stage with short deposition times (corresponding to thickness of up to 200 nm) formation of granular structures occurs. Beyond 200 nm, as the deposition time increases a second stage is observed, where the structures are developed both in width and in height, and have a six-folded pyramidal shape[15].

From the AFM images the surface roughness was determined as a function of film thickness. The results are shown in Figure 4. The RMS roughness of ZnO:Al thin films increases with increasing thickness due to the formation of a textured surface with pyramidal structures.

A similar dependence of the roughness on the thickness was also reported by Vasco et al.[15] (ZnO/InP), Seo et al.[21] (AGZO/glass) and Wang et al.[17] (AZO /Si/quartz). Vasco et al.[15], however, reported that the roughness of the ZnO/InP films continuously increases up to 240 nm in thickness and stabilizes from 400 nm due to development of the stepped facets in the pyramidal structures. Probably due to substrate bias polarization, similar stabilization was not observed here, at least until a thickness of 465nm. As also observed in the present study, Seo et al.[21] reported a sharp rise in roughness for thicknesses beyond 100 nm.

The main issues for the application of ZnO films as TCOs are high optical transmittance (above 80%) in the visible region and low resistivity (of about 10^{-3} to 10^{-4} Ω cm). In this context, Figure 5a shows the optical transmittance of ZnO:Al thin films as a function of wavelength for various thicknesses. Figure 5b shows transmission spectra of glass, ZnO and ZnO:Al films. Figure 5a shows a high optical transmittance (more than 85%) for the films of ZnO:Al in the visible range. According to Table 1, the refractive index for all films averaged 2.06 at 550 nm. Figure 5a also shows a decrease in optical transmittance from 1500 nm for the film with 465 nm thickness. The reduction in optical transmittance in the infrared region is most probably related to an increase in light reflection due to an increased charge carrier density. It is known that TCOs behave as metallic materials in the infrared region, and thus are reflective[2]. Furthermore, it is possible to observe in Figure 5b that the intrinsic ZnO film is transparent in the infrared region even when thicker than the ZnO:Al film.

From the optical transmission spectra it was possible to determine the value of the energy gap (E_G) using Equation 3[22].

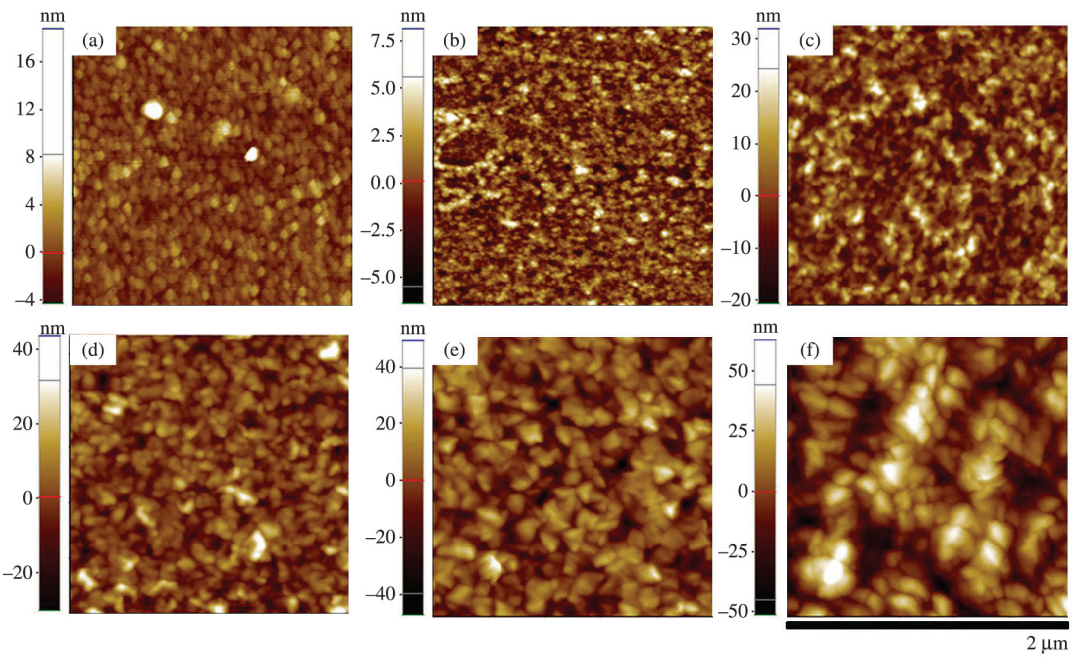

Figure 2. AFM images of glass substrate and ZnO:Al thin films grown to various thicknesses. (a) Glass substrate, (b) 25 nm, (c) 100 nm, (d) 165 nm, (e) 250 nm and (f) 465 nm.

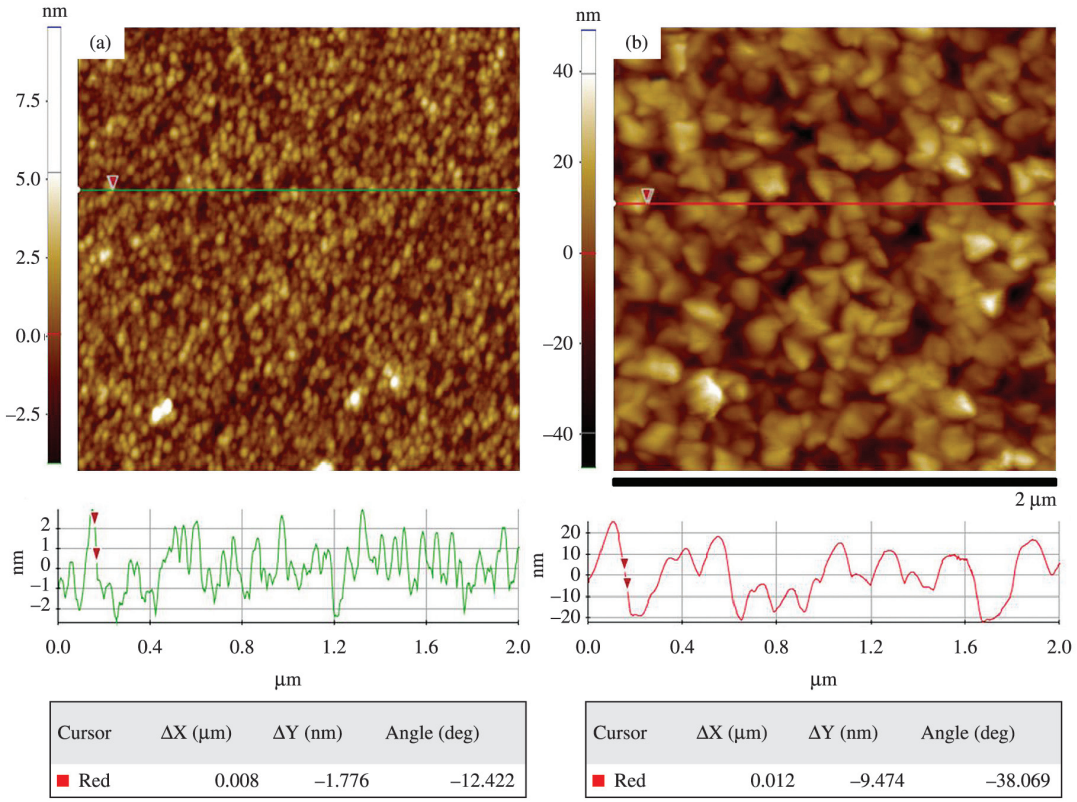

Figure 3. Surface AFM images (2 mm × 2 mm) and lateral profiles of the ZnO:Al thin films with (a) 50 nm and (b) 250 nm of thickness.

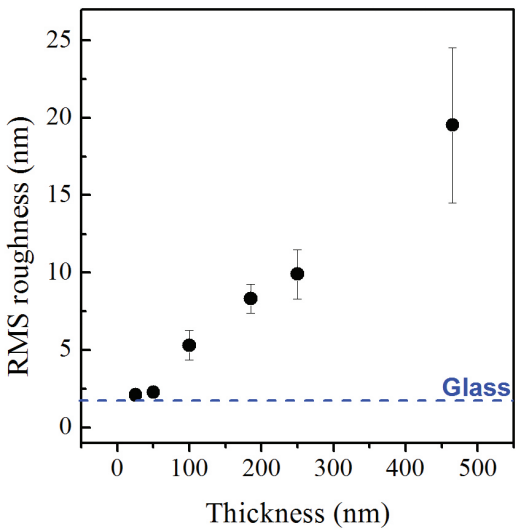

Figure 4. RMS roughness of the ZnO:Al films as a function of the film thickness.

$$\alpha h\nu = B(h\nu - E_g)^{1/2} \quad (3)$$

where α is the absorption coefficient, *hv* corresponds the photon energy, *B* is a band edge constant and the exponent of 1/2 corresponds to allowed direct transitions. As shown in Figure 6, the optical band gap can then be obtained from the intercept of $(ahv)^2$ versus *hv* for direct transitions. The values of the E_G were determined by extrapolating the linear portion of the curves to α = 0.

As derived from Figure 6, the energy gap of the intrinsic ZnO film of ~3.28 eV is in agreement with literature values. The film of ZnO:Al (465 nm) showed an increase in the gap to around 3.47 eV. This increase is related to the Moss Burstein effect[23,24]. When the number of critical charge carriers is exceeded in a n-type semiconductor, the Fermi level moves toward the conduction band by filling its lower states. Consequently an extension of the optical gap occurs and a higher excitation energy will be required for an electronic transition from the valence band to an unoccupied state of the conduction band[23,24]. The shift of the Fermi level to the conduction band can be described by Equation 4[23].

$$\Delta E_n = \left(\frac{h^2}{8m_c^*}\right)\left(\frac{3}{\pi}\right)^{2/3} N^{2/3} \quad (4)$$

where m_c^* is the effective mass of conduction, which for ZnO is equal to 0.38[23], *h* is Planck's constant, and *N* is the carrier density. Therefore, the carrier density of the doped film can be obtained knowing that the energy variation (ΔE_N) between the intrinsic ZnO film (3.28 eV) and the doped film (3.47 eV) is equal to 0.19 eV. It is known that the intrinsic ZnO film has a carrier density of 5.9×10^{18} cm^{-3}[23], and with doping the carrier density of the ZnO:Al film increases to 8.8×10^{19} cm^{-3}.

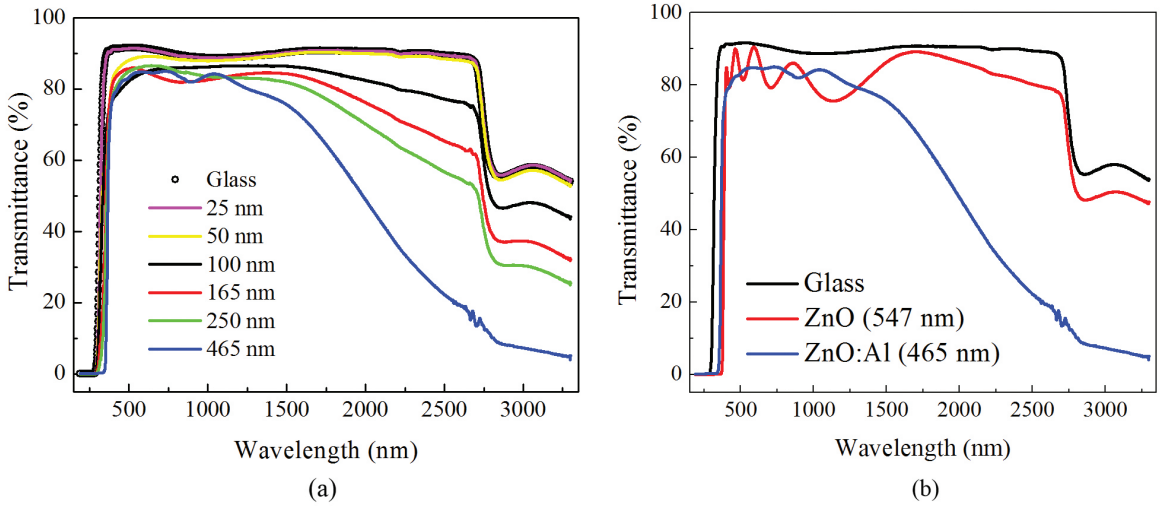

Figure 5. (a) Optical transmittance of ZnO:Al thin films as a function of film thickness. (b) Transmission spectra of the glass substrate, ZnO:Al (465 nm) and intrinsic ZnO (550 nm) thin films.

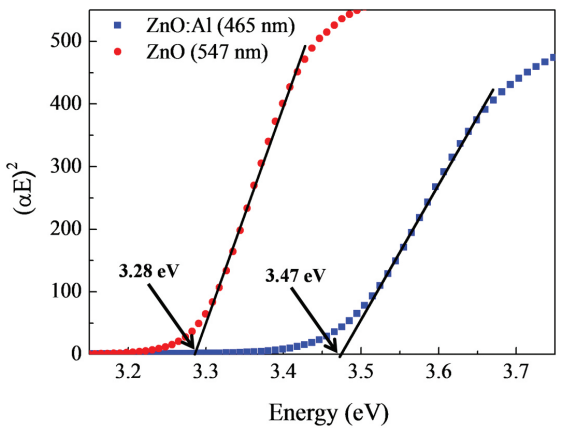

Figure 6. The energy gap of the ZnO:Al and intrinsic ZnO films estimated by the extrapolation of the linear part of the $(ahv)^2$ versus hv plots.

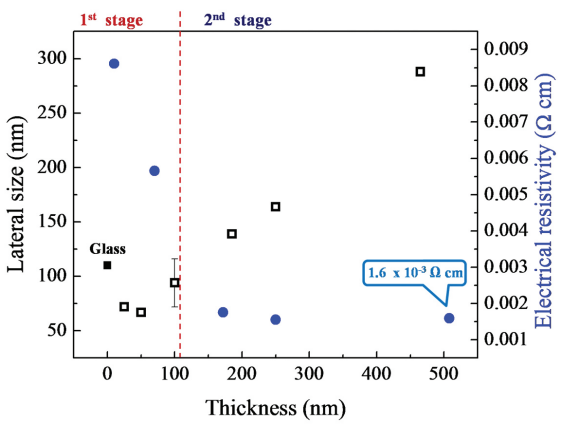

Figure 7. Lateral size calculated from a Lorentz fitting of the 2D power spectrum of 2 mm × 2 mm AFM images and electrical resistivity as a function of thickness.

Figure 7 shows the evolution of the lateral size of the grains, structures and the electrical resistivity with film thickness. The increase in charge carriers contributes to the decrease of the electrical resistivity. However, the resistivity depends on the thickness of the ZnO:Al films.

The Mayadas-Shatzkes theoretical model describes the dependence of resistivity on film thickness for polycrystalline thin films[25]. In his model, Mayadas-Shatzkes attributes the increase in resistivity to the scattering of electrons at grain boundaries[25]. Furthermore, Mayadas-Shatzkes assumes two cases for grains structures[25]. For films that show grain structures in column format, with a constant diameter, the resistivity of the material is independent of thickness[25]. For films that show structures with different grain diameters, however, the resistivity is dependent on the thickness[25]. As shown in Figure 7, the lateral size increases as a function of thickness. These results indicate that the films have grain structures with different diameters. Furthermore, the curve of electrical resistivity followed the trend expected for the second case cited above. Consequently, the mechanism that is influencing the resistivity of ZnO:Al films is the scattering of electrons at the grain boundaries.

According to Figure 7, a reduction of the lateral size for films with smaller thicknesses than 50 nm is observed. Films with smaller grain structures indicate an increase in defects at the grain boundaries, which increases the scattering of electrons and decreases the electronic mobility. For thicknesses above about 100 nm, however, an increase in lateral size occurs. This result indicates an improvement in crystallinity of the film and a decrease in the grain boundaries defects, with a consequent increase in electron mobility which in turn reduces the electrical resistivity.

From the data obtained of the carrier density (8.8×10^{19} cm^{-3}) and electrical resistivity (1.6×10^{-3} Ω cm) it was possible to determine the value of the electron mobility (m_E) for the thicker ZnO:Al film (550 nm) using Equation 5.

$$\mu_e = \frac{1}{\rho n e} \quad (5)$$

were ρ is the electrical resistivity, *n* is the number of charge carriers and *e* corresponds to the electronic charge. The electron mobility of ZnO:Al film is ~ 44 cm^2/Vs.

The corresponding resistivity curve, however, tends to stabilize at 1.6×10^{-3} Ω cm and, therefore, the electron mobility stabilizes at 44 cm^2/V.s. This limitation may be caused by defects in the crystal lattice of ZnO related to the aluminum atoms. These defects act as electron scattering centers and reduce the electron mobility. Indeed, the electron mobility is predicted to be about 50 cm^2/Vs for an aluminum doping concentration of 10^{20} cm^{-3} when the ionized impurity scattering mechanism is considered[1].

4. Conclusions

ZnO:Al thin films were deposited onto glass substrates by RF magnetron sputtering. Surface morphology exhibits a transition between small grain structures of granular shape to grain structures of pyramidal shape. The XRD results showed that the films have a preferred crystal orientation in the (002) plane, along the *c*-axis perpendicular to the substrate surface. As the thickness of the films increases an increase in lateral grain size occurs and, consequently, an improvement in the crystallinity is obtained. On the other hand, the resistivity tends to decrease with increasing thickness to a minimum value of 1.6×10^{-3} Ω cm. In addition, the films exhibited a good optical transmittance of more than 85% in the visible region.

Acknowledgements

The authors acknowledge the financial support of the Brazilian agencies FAPESP (2008/53311-5, 2011/21345-0) and CNPq (555774/2010-4, 301622/2012-4).

References

1. Ellmer K, Klein A and Rech B, editors. *Transparent conductive zinc oxide: basics and applications in thin film solar cells*. New York: Springer; 2008. Springer Series in Materials Science, v. 104. http://dx.doi.org/10.1007/978-3-540-73612-7.
2. Ginley DS, Hosono H and Paine DC, editors. *Handbook of transparent conductors*. New York: Springer; 2010.
3. Liu H, Avrutin V, Izyumskaya N, Özgür Ü and Morkoç H. Transparent conducting oxides for electrode applications in light emitting and absorbing devices. *Superlattices and Microstructures*. 2010; 48(5):458-484. http://dx.doi.org/10.1016/j.spmi.2010.08.011.
4. Zhu H, Mai Y, Wan M, Gao J, Wang Y, He T, et al. Study of back reflectors for thin film silicon solar cells. *Thin Solid Films*. 2013; 539:284-289. http://dx.doi.org/10.1016/j.tsf.2013.05.019.
5. Tseng CA, Lin JC, Weng WH and Lin CC. Photoelectron spectroscopy and optical properties of Al-Doped ZnO films prepared by sputtering with radio frequency power applied to Al target. *Japanese Journal of Applied Physics*. 2013; 52(2R):025801. http://dx.doi.org/10.7567/JJAP.52.025801.
6. Fazio E, Patanè S, Scibilia S, Mezzasalma AM, Mondio G, Neri F, et al. Structural and optical properties of pulsed laser deposited ZnO thin films. *Current Applied Physics*. 2013; 13(4):710-716. http://dx.doi.org/10.1016/j.cap.2012.11.010.
7. Ding K, Hu QC, Wang X, Zhang JY, Lin WW, Lin CS, et al. Aluminum doping induced columnar growth of homoepitaxial ZnO films by metalorganic chemical vapor deposition. *Applied Physics Letters*. 2013; 103(14):141907. http://dx.doi.org/10.1063/1.4824116.
8. Ortel M, Balster T and Wagner V. Chemical composition and temperature dependent performance of ZnO-thin film transistors deposited by pulsed and continuous spray pyrolysis. *Journal of Applied Physics*. 2013; 114(23):234502. http://dx.doi.org/10.1063/1.4846736.
9. Ammaih Y, Lfakir A, Hartiti B, Ridah A, Thevenin P and Siadat M. Structural, optical and electrical properties of ZnO: Al thin films for optoelectronic applications. *Optical and Quantum Electronics*. 2014; 46(1):229-234. http://dx.doi.org/10.1007/s11082-013-9757-2.
10. Kim KW, Son HS, Choi NJ, Kim J and Lee SN. Growth and characterization of polar and nonpolar ZnO film grown on sapphire substrates by using atomic layer deposition. *Thin Solid Films*. 2013; 546:114-117. http://dx.doi.org/10.1016/j.tsf.2013.03.071.
11. Bikowski A, Welzel T and Ellmer K. The correlation between the radial distribution of high-energetic ions and the structural as well as electrical properties of magnetron sputtered ZnO: Al films. *Journal of Applied Physics*. 2013; 114(22):223716. http://dx.doi.org/10.1063/1.4840975.
12. Wu HW, Yang RY, Hsiung CM and Chu CH. Characterization of aluminum-doped zinc oxide thin films by RF magnetron sputtering at different substrate temperature and sputtering power. *Journal of Materials Science Materials in Electronics*. 2013; 24(1):166-171. http://dx.doi.org/10.1007/s10854-012-0769-7.
13. Karabacak T. Thin-film growth dynamics with shadowing and re-emission effects. *Journal of Nanophotonics*. 2011; 5(1):052501. http://dx.doi.org/10.1117/1.3543822.
14. Kajikawa Y. Texture development of non-epitaxial polycrystalline ZnO films. *Journal of Crystal Growth*. 2006; 289(1):387-394. http://dx.doi.org/10.1016/j.jcrysgro.2005.11.089.
15. Vasco E, Zaldo C and Vázquez L. Growth evolution of ZnO films deposited by pulsed laser ablation. *Journal of Physics Condensed Matter*. 2001; 13(28):L663-L672. http://dx.doi.org/10.1088/0953-8984/13/28/102.
16. Chen XL, Wang F, Geng XH, Zhang DK, Wei CC, Zhang XD, et al. Natively textured surface Al-doped ZnO-TCO layers with gradual oxygen growth for thin film solar cells via magnetron sputtering. *Applied Surface Science*. 2012; 258(8):4092-4096. http://dx.doi.org/10.1016/j.apsusc.2011.12.061.
17. Wang F, Wu MZ, Wang YY, Yu YM, Wu XM and Zhuge LJ. Influence of thickness and annealing temperature on the electrical, optical and structural properties of AZO thin films. *Vacuum*. 2013; 89:127-131. http://dx.doi.org/10.1016/j.vacuum.2012.02.040.
18. Betz U, Kharrazi Olsson M, Marthy J, Escolá MF and Atamny F. Thin films engineering of indium tin oxide: Large area flat panel displays application. *Surface and Coatings Technology*. 2006; 200(20-21):5751-5759. http://dx.doi.org/10.1016/j.surfcoat.2005.08.144.
19. Rosa AM, da Silva EP, Amorim E, Chaves M, Catto AC, Lisboa-Filho PN, et al. Growth evolution of ZnO thin films

deposited by RF magnetron sputtering. *Journal of Physics: Conference Series*. 2012; 370(1):012020. http://dx.doi.org/10.1088/1742-6596/370/1/012020.

20. Avril L, Guaino P, Maseri F, Muthukaruppasamy K and Pireaux JJ. Correlation between the electrical and structural properties of aluminium-doped ZnO thin films obtained by direct current magnetron sputtering. *Journal of Physics: Conference Series*. 2013; 417(1):012011. http://dx.doi.org/10.1088/1742-6596/417/1/012011.
21. Seo K-W, Shin H-S, Lee J-H, Chung K-B and Kim H-K. The effects of thickness on the electrical, optical, structural and morphological properties of Al and Ga co-doped ZnO films grown by linear facing target sputtering. *Vacuum*. 2014; 101:250-256. http://dx.doi.org/10.1016/j.vacuum.2013.09.009.
22. Vinodkumar R, Navas I, Chalana SR, Gopchandran KG, Ganesan V, Philip R, et al. Highly conductive and transparent laser ablated nanostructured Al: ZnO thin films. *Applied Surface Science*. 2010; 257(3):708-716. http://dx.doi.org/10.1016/j.apsusc.2010.07.044.
23. Roth AP, Webb JB and Williams DF. Absorption edge shift in ZnO thin films at high carrier densities. *Solid State Communications*. 1981; 39(12):1269-1271. http://dx.doi.org/10.1016/0038-1098(81)90224-6.
24. Singh B, Khan ZA, Khan I and Ghosh S. Highly conducting zinc oxide thin films achieved without postgrowth annealing. *Applied Physics Letters*. 2010; 97(24):241903. http://dx.doi.org/10.1063/1.3525575.
25. Philipp M. *Electrical transport and scattering mechanisms in thin silver films for thermally insulating glazing*. [Dissertation]. Dresden: Leibniz Institut für Festkörper-und Werkstofforschung (IFW) and Institut des NanoSciences de Paris (INSP); 2011.